Sensors and Actuators B 232 (2016) 28–36

Contents lists available at ScienceDirect

Sensors and Actuators B: Chemical

journal homepage: www.elsevier.com/locate/snb

A novel rhodamine-based colorimetric and fluorescent sensor for Hg^{2+} in water matrix and living cell

Miaomiao Hong[a,b], Xiangyu Lu[a,b], Yuhua Chen[c], Dongmei Xu[a,b,*]

[a] College of Chemistry, Chemical Engineering and Materials Science, Soochow University, Suzhou, Jiangsu 215123, China
[b] Jiangsu Key Laboratory of Advanced Functional Polymer Design and Application, Soochow University, Suzhou, Jiangsu 215123, China
[c] College of Pre-clinical Medical and Biological Science, Soochow University, Suzhou 215123, China

ARTICLE INFO

Article history:
Received 25 January 2016
Received in revised form 21 March 2016
Accepted 23 March 2016
Available online 24 March 2016

Keywords:
Rhodamine
Colorimetric sensor
Fluorescent sensor
Solid support sensor
Hg^{2+}
Cell imaging

ABSTRACT

A novel rhodamine-based colorimetric and fluorescent sensor for Hg^{2+} was reported. In CH_3CN/H_2O (1/99, v/v), the sensor showed high selectivity and sensitivity to Hg^{2+} by an emerging absorption peak at 565 nm and a 32-fold fluorescence enhancement at 586 nm with vivid color changes. The absorbance and fluorescence maxima increased linearly with the concentration of Hg^{2+} in the range of 0–90 μM. The colorimetric and fluorescent detection limits were 6.36 μM and 60.78 nM respectively. The sensor could work in a nearly neutral pH span of 6.01–8.57 and exhibited excellent interference immunity and low cytotoxicity. A 1:2 sensor-Hg^{2+} complex formed with a binding constant of $2.89 \times 10^8\ M^{-2}$. A new sensing mechanism was proposed. The sensor was successfully applied in real sample assay and living cell imaging. Furthermore, the sensor could be supported in low cost cellulose discs for signaling Hg^{2+} in 100% aqueous solution.

1. Introduction

Mercury is widely present in air, water and soil as a result of fossil fuel combustion, solid waste incineration, chemical industry, mining industry and metal smelting. As we know, mercury is one of the most dangerous and toxic heavy metals due to its high affinity to thiol groups in enzymes and proteins, destroying cell's function and consequently causing a large number of health problems, such as cognitive disorder, brain and neurological damage, even in low concentration [1,2]. Therefore, the development of simple methods for monitoring Hg^{2+} in the environment and biological system is critical.

Fluorescent sensors are highly selective, highly sensitive, maneuverable, low-cost, and suitable for in-situ and real-time monitoring, so they are very active in the field of heavy metal ions signaling currently [3–5]. A large number of colorimetric and fluorescent sensors for Hg^{2+} have been reported [2,6–9]. However, some of them were with complicated structure and difficult to synthesize [10,11], others could only respond to Hg^{2+} in organic media [12,13], or suffered from poor sensing properties including selectivity, sensitivity, interference immunity, and practicability [14,15]. Hg^{2+} sensors with satisfactory comprehensive performance are scarce and their design and synthesis are very attractive but greatly challenging. Among the various chemosensors, rhodamine derivatives are regarded as unique platforms because their spiro-ring opening processes can induce striking "off-on" colorimetric and fluorescent changes and their sensing properties can be tuned by the modification of the parent structure [16–21]. The reported irreversible rhodamine-based Hg^{2+} sensors mainly sensed Hg^{2+} through Hg^{2+}-induced spirolactam-ring opening, followed by two kinds of typical chemical reactions. The first is hydrolysis to generate carboxy derivative [20,21], the second is the production of a new five-numbered heterocycle [22,23]. The exploration of new sensing mechanism is important for the development of new rhodamine-based Hg^{2+} sensors with excellent comprehensive performance.

In this paper, we designed and synthesized a novel rhodamine-based Hg^{2+} sensor with excellent overall performance, and a new interaction way between $Hg^{2+}$and the sensor was proposed and verified.

2. Experimental

2.1. Reagents and instruments

Rhodamine B (RB) was purchased from Shanghai SSS Reagent Co., Ltd. (Shanghai, China). Tris(2-aminoethyl)amine (TAEA) was bought from Acros Organics (Beijing, China). Phenyl isothiocyanate

* Corresponding author at: College of Chemistry, Chemical Engineering and Materials Science, Soochow University, Suzhou, Jiangsu 215123, China.
E-mail address: xdm.sd@163.com (D. Xu).

http://dx.doi.org/10.1016/j.snb.2016.03.125
0925-4005/

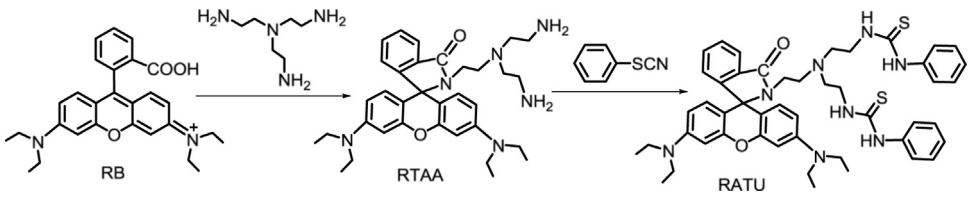

Scheme 1. Synthetic route of RATU.

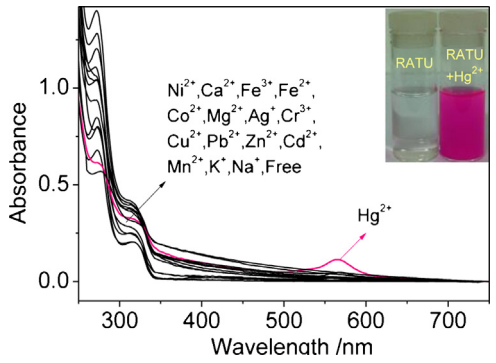

Fig. 1. UV–vis absorption spectra of RATU in the absence and presence of various cations. Solvent: CH_3CN/H_2O (1/99, v/v), c: 30 μM for RATU, 210 μM for metal ions.

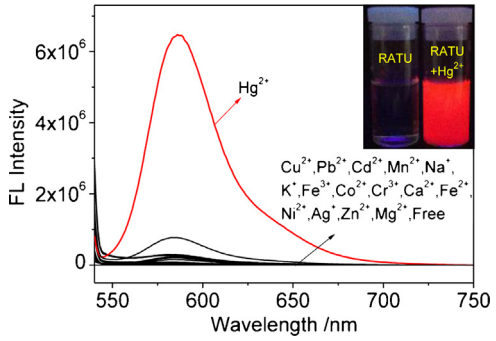

Fig. 2. Fluorescence spectra of RATU in the absence and presence of various cations. Solvent: CH_3CN/H_2O (1/99, v/v), c: 30 μM for RATU, 210 μM for metal ions. λ_{ex}: 520 nm, slit width: 10 nm.

(PITC) was purchased from Aladdin Industries Inc. (Shanghai, China). Metal ion like Na^+, K^+, Mg^{2+}, Ca^{2+}, Fe^{3+}, Fe^{2+}, Zn^{2+}, Cr^{3+}, Pb^{2+}, Ni^{2+}, Co^{2+}, Cd^{2+}, Ag^+ and Hg^{2+} were provided by their nitrate or chloride salts except Cu^{2+} and Mn^{2+} were used as their sulphate salts. The salts and the solvents were commodities of Sinopharm Chemical Reagent Co., Ltd. (Shanghai, China). All the reagents were of analytical grade. The solvents used in synthesis were of analytical grade, others were spectroscopic grade. All were used as received.

Mass spectrum was recorded on an Agilent 6220 Quadruple LC/MS (Agilent Co., USA) in ESI positive mode unless otherwise specified. IR spectra were carried out on a Nicolet Magan-550 spectrometer (Nicolet Co., USA). ^1H NMR and ^{13}C NMR spectra were performed in $CDCl_3$ on a 400 and a 300 MHz Varian Unity Inova spectrometers (Varian Co., USA) respectively. Elemental analysis was obtained on a Carlo-Erba EA1110CHNO-S elemental analyzer (Carlo-Erba Co., Italy). Absorption and fluorescence spectra were tested on a U-3900 spectrophotometer (Perkin-Elmer Co., USA) and a Fluoromax-4 spectrofluorometer (HORIBA Jobin Yvon Co., France), respectively. pH values were measured with a Mettler-Toledo FE20 pH meter (Mettler-Toledo Co., USA). Melting point was determined on an X-6 Microscopic melting point tester (Beijing Taike Instrument Co., Ltd., China). Color and fluorescence photos were taken by an iphone mobile (Apple Inc., USA). Cell images were done on a Nikon Eclipse Ti inverted fluorescence microscope (Nikon Instruments Inc., Japan) excited by green light. Viability of the cells was tested by a MUSE Smart Touch cell analyzer (Nikon Merck Drugs & Biotechnology Inc., Germany).

2.2. Synthesis of the sensor (RATU)

The novel rhodamine derivative (RATU) was synthesized by two-step reactions between rhodamine B (RB), tris(2-aminoethyl)amine (TAEA) and phenyl isothiocyanate (PITC) (Scheme 1). RB reacted with TAEA to get the intermediate (RTAA) following the references [24]. Then to a stirring CH_3CN (10 mL) solution of RTAA (0.2 g, 0.35 mmol), PITC (167 μL, 1.4 mmol) was added dropwise and reacted at room temperature for 6 h. Next the solvent was removed under reduced pressure. The residue was separated by sillica-gel column chromatography with ethyl acetate/petroleum ether (1/2, v/v) as an eluent to afford a white solid RATU (49.7 mg). Yield, 57%. m.p. 141.7 °C. ^1H NMR (400 MHz, $CDCl_3$) (Fig. S1, Supporting information (ESI)), δ: 1.17 (12H, *t*, *J* = 7.2 Hz), 2.03 (2H, t, *J* = 4.4 Hz), 2.48–2.50 (6H, m), 3.10 (2H, t, *J* = 3.6 Hz), 3.36 (8H, t, *J* = 7.2 Hz), 3.49–3.53 (4H, m), 6.31 (2H, s), 6.34 (2H, d, *J* = 8.4 Hz), 6.37–6.39 (4H, m), 7.09–7.15 (2H, m), 7.29–7.33 (4H, m), 7.39 (4H, d, *J* = 8.4 Hz), 7.49–7.53 (1H, m), 7.64 (1H, d, *J* = 7.6 Hz), 8.23 (2H, s); ^{13}C NMR (75 MHz, $CDCl_3$) (Fig. S2, ESI), δ: 180.66, 168.91, 153.54, 152.79, 149.00, 138.16, 133.18, 130.74, 129.11, 128.64, 128.21, 125.34, 124.12, 123.66, 122.32, 108.52, 104.42, 97.37, 66.47, 52.92, 44.22, 42.32, 39.31, 12.47; ESI–MS (Fig. S3, ESI): $[M+H]^+$ = 841.41, $[M+Na]^+$ = 863.39; Elemental analysis data as calculated for $C_{48}H_{56}N_8O_2S_2$ (%): C, 68.54; N, 13.32; H, 6.71. Found (%): C, 68.99; N, 13.34; H, 6.83. FTIR (cm^{-1}) (Fig. S4, ESI): ν(NH) 3352.19; ν(CH_3 and CH_2) 2974.16, 2920.15 cm^{-1}, 2868.07; ν(C=O) 1668.38; ν(ArH) 1616.30, 1517.94, 1467.79; ν(C=S) 1118.68.

2.3. Testing and calculating methods

2.3.1. General procedure for spectral study

The stock solution of RATU (3×10^{-3} M) was prepared in CH_3CN. Stock solutions of metal salt and EDTA (1×10^{-2} M) were prepared in deionized water (H_2O). When studying the selectivity of RATU to Hg^{2+}, 100 μL stock solution of RATU in each of 16 volumetric flasks was mixed with 210 μL of metal ion stock solution (Na^+, K^+, Mg^{2+}, Ca^{2+}, Fe^{3+}, Fe^{2+}, Cu^{2+}, Zn^{2+}, Cr^{3+}, Mn^{2+}, Pb^{2+}, Ni^{2+}, Co^{2+}, Cd^{2+}, Ag^+ or Hg^{2+}) respectively. To exam the effects of the concentration of Hg^{2+}, each 100 μL stock solution of RATU in several 10 mL volumetric flasks was mixed with various concentrations of Hg^{2+} (from 0 to 210 μM) respectively. In the anti-interference experiment, 150 μL of Na^+, K^+, Mg^{2+}, Fe^{3+}, Cu^{2+}, Pb^{2+}, Ni^{2+}, Cr^{3+}, Fe^{2+}, and Cd^{2+}, and 100 μL of Ca^{2+}, Mn^{2+}, Zn^{2+}, and Co^{2+} were added to the 10 mL volumetric flasks containing RATU (100 μL) and Hg^{2+} (210 μL) individually. In the Job's plot experiment, a series of RATU-Hg^{2+} solutions with 30 μM total concentration of Hg^{2+} and RATU (molar fraction of Hg^{2+} varied from 0 to 1) and the corresponding blank RATU solutions were prepared. In the study of reversibility, stock solution of RATU (100 μL) was mixed with Hg^{2+} (210 μL) in 10 mL volumetric flasks and the fluorescence spectra were assayed. Then, excess EDTA (500 μL) was introduced and the fluorescence

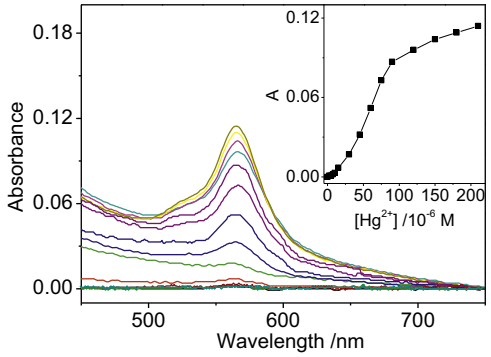

Fig. 3. UV–vis absorbance spectra of RATU (30 μM) with various concentrations of Hg^{2+}. Solvent: CH_3CN/H_2O (1/99, v/v), From bottom to top, the concentration of Hg^{2+}: 0, 2.5, 5, 7.5, 10, 15, 30, 45, 60, 75, 90, 120, 150, 180, 210 μM. Insets: the relationship between the absorbance maxima (A) at 565 nm and the concentration of Hg^{2+}.

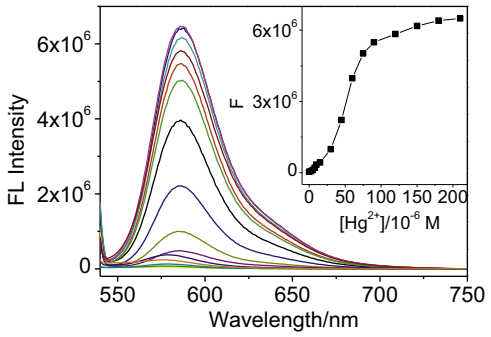

Fig. 4. Fluorescence spectra of RATU (30 μM) with various concentrations of Hg^{2+}. Solvent: CH_3CN/H_2O (1/99, v/v), λ_{ex}: 520 nm, slit width: 10 nm. From bottom to top, the concentration of Hg^{2+}: 0, 2.5, 5, 7.5, 10, 15, 30, 45, 60, 75, 90, 120, 150, 180, 210 μM. Insets: The relationship between the maximal fluorescence intensity (F) at 586 nm and the concentration of Hg^{2+}.

spectra were recorded again. All the samples were diluted with H_2O to volume before test. The UV–vis absorption and fluorescence spectra were recorded after 90 min at 20 °C with an excitation wavelength of 520 nm and a slit width of 10 nm. pH was adjusted by 0.1 M HCl and 0.1 M NaOH aqueous solutions.

2.3.2. Detection limit

The detection limit (3S/K) [25] was calculated based on UV–vis absorption and fluorescence titration, where S is the standard deviation of the intensity of the free sensor solution, K is the slope of the linear fitting lines of the titration data (the absorbance and the fluorescence intensity with Hg^{2+} concentration). To determine S, the absorption and emission intensity of the free sensor solution was measured 5 times respectively.

2.3.3. Binding constant

The binding constant for RATU-Hg^{2+} was obtained with a Benesi-Hildebrand Eq. (1) [26]. where F, F_{min}, F_{max} were the fluorescence intensity of RATU at a certain concentration of Hg^{2+}, in the absence of Hg^{2+} and at saturated concentration of Hg^{2+}, respectively. K was the binding constant.

$$\frac{1}{F-F_{min}} = \frac{1}{F_{max}-F_{min}}\left[\frac{1}{K\left[Hg^{2+}\right]^2}+1\right] \quad (1)$$

2.3.4. IR spectra test in the study of the sensing mechanism

The solvents in the CH_3CN/H_2O (1/99, v/v) solution of RATU (30 μM) and RATU (30 μM)-Hg^{2+} (210 μM) used for UV–vis absorption and fluorescence test were evaporated under reduced pressure. The remains were dried in vacuum to constant weight and their IR spectra were collected respectively by routine method.

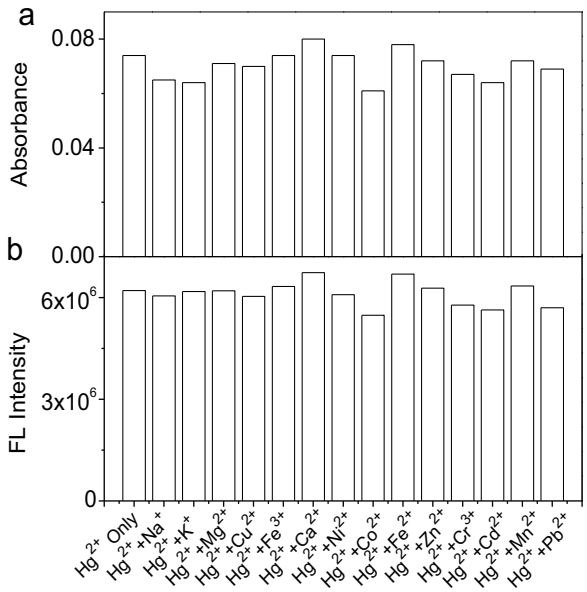

Fig. 5. Effects of coexisting ions on the UV–vis absorption maxima at 565 nm (a) and the fluorescence maxima at 586 nm (b) of the RATU-Hg^{2+} solutions. Solvent: CH_3CN/H_2O (1/99, v/v), c: 30 μM for RATU, 210 μM for Hg^{2+}, 150 μM for Na^+, K^+, Mg^{2+}, Fe^{3+}, Cu^{2+}, Pb^{2+}, Ni^{2+}, Cr^{3+}, Fe^{2+} and Cd^{2+}, 100 μM for Ca^{2+}, Mn^{2+}, Zn^{2+} and Co^{2+}.

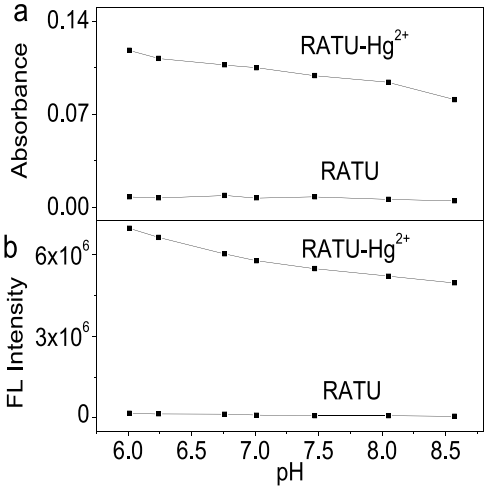

Fig. 6. Effect of pH on the absorbance at 565 nm (a) and the fluorescence intensity at 586 nm (b) of RATU (30 μM) in the absence and presence of Hg^{2+} (210 μM) in CH_3CN/H_2O (1/99, v/v), pH: 6.01, 6.24, 6.76, 7.01, 7.47, 8.05 and 8.57. λ_{ex}: 520 nm, slit width: 10 nm.

2.3.5. Real samples analysis

For real sample analysis, 1 mL tap water or pool water was put into a 10 mL volumetric flask. Next, RATU (100 μL) and Hg^{2+} (25 μL, 75 μL or 90 μL) were added, diluted with H_2O to volume, and the fluorescence spectrum was assayed. To determine the relative standard deviation (RSD), three samples were measured for each Hg^{2+} concentration.

2.3.6. Cell culture and imaging

sf9 cells were seeded in a 24-well plate at a density of 1×10^4 cells per well in culture media TC-100 with 10% foetal bovine serum

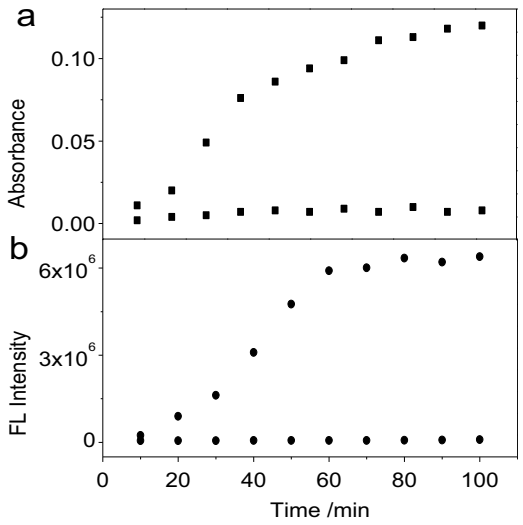

Fig. 7. Time response the absorption (a) and fluorescence maxima (b) of RATU to Hg^{2+}. Solvent: CH_3CN/H_2O (1/99, v/v), c: 30 μM for RATU, 210 μM for Hg^{2+}, λ_{ex}: 520 nm, slit width: 10 nm.

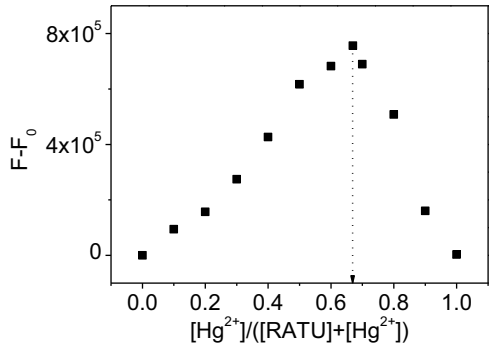

Fig. 8. Job's plot for Hg^{2+} versus RATU. Total concentration ([RATU] + [Hg^{2+}]): 30 μM, F_0 and F: fluorescence maxima before and after addition of Hg^{2+} at 586 nm, respectively. λ_{ex}: 520 nm, slit width: 10 nm.

(Sigma) for 24 h at 27 °C. Then, the cells in 9 wells were equally split into three groups. Group 1 was left as the controls. Group 2 and 3 were incubated with 9 and 12 μL Hg^{2+} for 40 min, respectively. Next, 10, 15 or 20 μL of RATU was added into 3 wells in group 2 (and group 3) respectively. After incubated for another 40 min, the cells were observed and imaged on a Nikon Eclipse Ti inverted fluorescence microscope excited with green light.

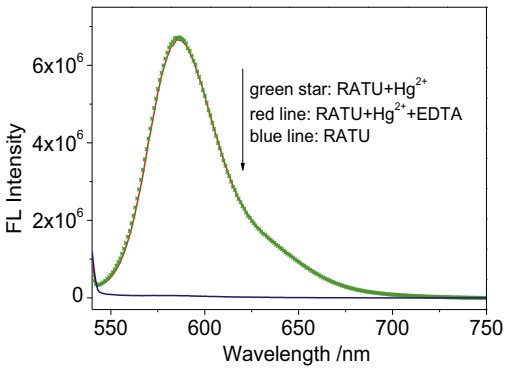

Fig. 9. Reversibility of the fluorescence detection of Hg^{2+} with RATU. Solvent: CH_3CN/H_2O (1/99, v/v), c: 30 μM for RATU, 210 μM for Hg^{2+}. λ_{ex}: 520 nm, slit width: 10 nm.

2.3.7. Cytotoxicity assays

The stock solutions of RATU (30, 45 and 60 mM) were prepared in CH_3CN. sf-9 cells (1 mL, 1×10^4 cells per dish) in culture media TC-100 with 10% foetal bovine serum were cultured in each of 12 culture dishes for 24 h at 27 °C and separated into four groups. Group 1 was left as the control. Group 2, 3 and 4 were induced 30, 45 and 60 mM of RATU (1 μL) respectively. The cells were incubated at 27 °C for another 24 h. Then, Muse detection reagent was added into the cells away from light. After 5 min the percentage of live cells in total cells was tested automatically by a MUSE Smart Touch cell analyzer. The viability was expressed as the percentage compared with the control.

3. Results and discussion

3.1. Selectivity of RATU to Hg^{2+}

The interaction of RATU with cations such as Na^+, K^+, Mg^{2+}, Ca^{2+}, Fe^{3+}, Fe^{2+}, Zn^{2+}, Cr^{3+}, Pb^{2+}, Ni^{2+}, Co^{2+}, Cd^{2+}, Ag^+ and Hg^{2+} was examined by both UV–vis absorption and fluorescence spectroscopy techniques in CH_3CN/H_2O(1/99, v/v). The UV–vis absorption spectra (Fig. 1) showed that only addition of Hg^{2+} gave rise to an emerging peak near 565 nm companied by a naked-eye observed color change from colorless to red. Other metal cations did not induce significant changes. Similarly, only Hg^{2+} aroused a 32-fold fluorescence enhancement at 586 nm and brought a shining red fluorescence to the non-emissive dark RATU solution (Fig. 2). These results indicate that RATU is highly selective and sensitive to Hg^{2+} and may be a potential colorimetric and fluorescent sensor for Hg^{2+} in CH_3CN/H_2O (1/99, v/v).

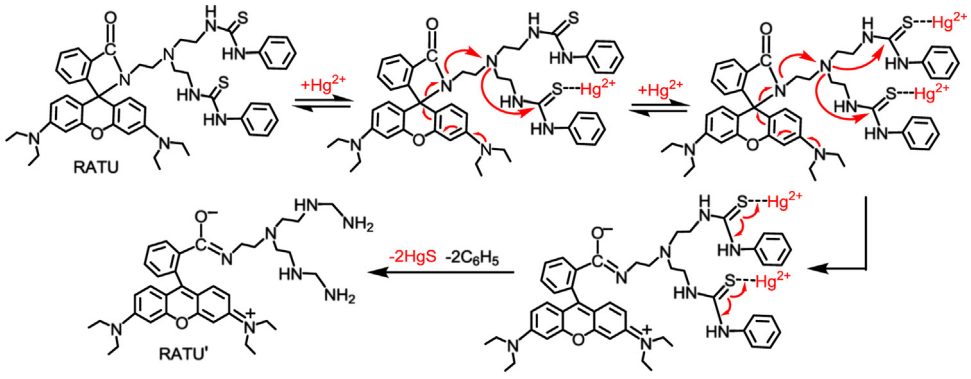

Scheme 2. Proposed sensing mechanism of RATU for Hg^{2+}.

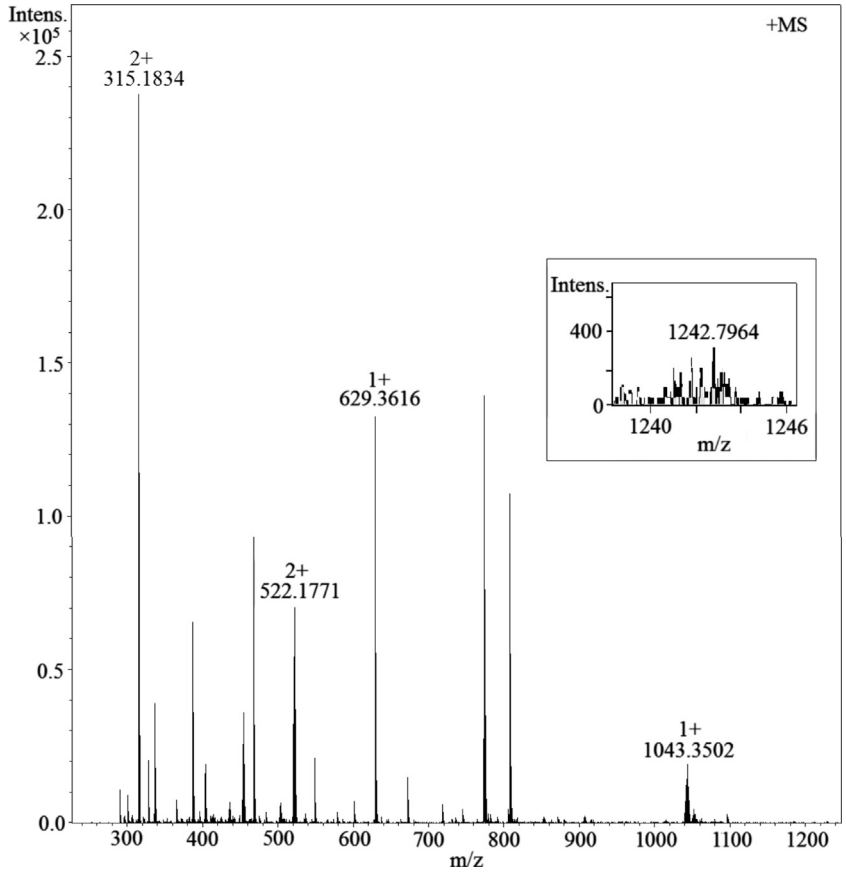

Fig. 10. LC–MS of RATU-Hg^{2+} recorded by a Brukermicro TOF-QIII LC/MS (Bruker Daltonics Co., Germany).

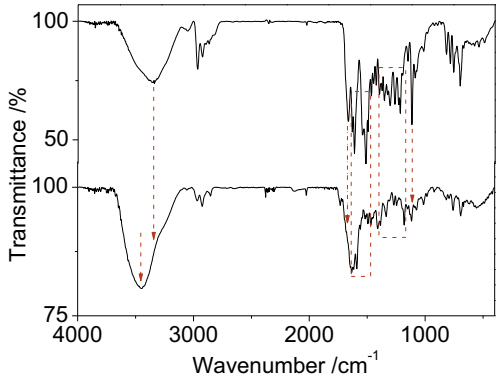

Fig. 11. IR spectra of (a) RATU and (b) RATU-Hg^{2+}.

Table 1
Determination of Hg^{2+} in tap water and pool water (n = 3).

Sample	Hg^{2+} added (μM)	Hg^{2+} found (μM)	Recovery (%)	RSD[a] (%)
Tap water	25.0	25.1	100.4	0.39
	75.0	76.7	102.3	1.18
	90.0	88.2	98.0	1.79
Pool water	25.0	24.7	98.8	0.82
	75.0	74.2	98.9	0.90
	90.0	91.6	101.8	0.94

[a] RSD is relative standard deviation.

3.2. Dependency of RATU's spectra on Hg^{2+} concentration

To investigate the possibility of RATU used as a colorimetric and fluorescent sensor for Hg^{2+}, titration experiments in CH_3CN/H_2O (1/99, v/v) were performed. The absorption intensity of the RATU solutions gradually enhanced with the addition of various concentration of Hg^{2+} (from 0 to 210 μM) (Fig. 3). Moreover, the absorbance maxima at 565 nm increased linearly with the concentration of Hg^{2+} in the range of 0–90 μM (Inset in Fig. 3). The blank RATU solution was almost non-emissive. Upon addition of Hg^{2+}, a new band centered at 586 nm appeared, and its intensity rose with the increasing Hg^{2+} concentrations (Fig. 4). The linear response of the fluorescence intensity toward Hg^{2+} was also in the range of Hg^{2+} concentration 0–90 μM (Inset in Fig. 4). The detection limit evaluated from the colorimetric and fluorescent titration was 6.36 μM and 60.78 nM respectively. The fact that the UV–vis absorption and fluorescence intensity of the RATU solutions depended on the Hg^{2+} concentration quantitatively upholds RATU as a colorimetric and fluorescent sensor for Hg^{2+}.

3.3. Anti-interference of RATU for detecting Hg^{2+}

To know the disturbance of the coexisting ions to the detection of Hg^{2+} with RATU, Na^+, K^+, Mg^{2+}, Ca^{2+}, Fe^{3+}, Fe^{2+}, Cu^{2+}, Zn^{2+}, Cr^{3+}, Mn^{2+}, Pb^{2+}, Ni^{2+}, Co^{2+}, and Cd^{2+} were introduced into the CH_3CN/H_2O (1/99, v/v) solutions of RATU-Hg^{2+}, and UV–vis absorption and fluorescence spectra were recorded. It can be seen that the added competition ions had negligible influence on the absorption (Fig. 5a) and fluorescence (Fig. 5b) maxima of the RATU-Hg^{2+} solutions, which indicated the excellent anti-interference performance of RATU for monitoring Hg^{2+}.

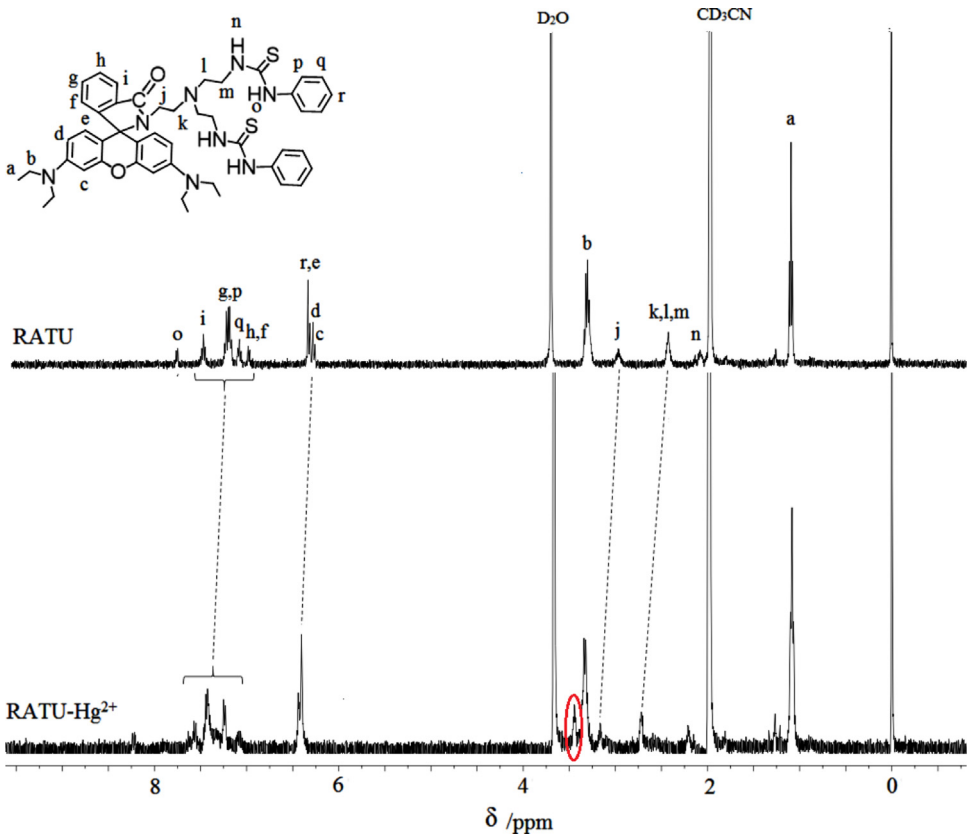

Fig. 12. ^{1}H NMR spectra of RATU and RATU-Hg^{2+} in CD_3CN-D_2O (2/1, v/v) (400 MHz).

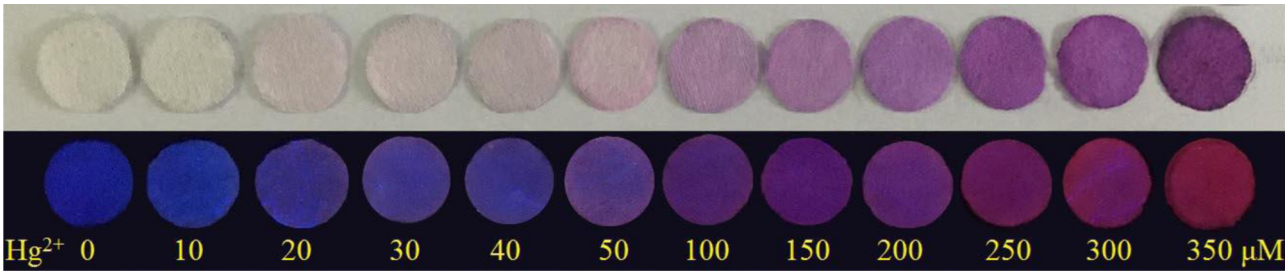

Fig. 13. Color changes of cellulose discs containing RATU (113 μM) after immersing (60 min) in water solutions containing increasing amounts of Hg^{2+} (0–350 μM). Top: under natural right, bottom: under a ZF-20D camera obscura ultraviolet analyzer (Shanghai Yuzheng Instrument Equipment Co., Ltd.).

3.4. Effect of pH on the detection

In order to investigate if RATU can be applied in nearly neutral pH scope, UV–vis absorption and fluorescence spectra of a series of RATU and RATU-Hg^{2+} CH_3CN/H_2O (1/99, v/v) solutions with different pH values were tested. As shown in Fig. 6, the absorbance and the fluorescence intensity of RATU-Hg^{2+} showed a small decrease with the increase of pH between 6.01 and 8.57, while those of the blank RATU almost kept stable at a very low level. The absorbance and the fluorescence intensity of RATU-Hg^{2+} were much higher than those of the corresponding blank RATU. Thus, RATU can colorimetrically and fluorimetrically detect Hg^{2+} in a pH span of 6.01–8.57 which was suitable for ecological and biological systems.

3.5. Time-dependence of the detection

Reaction time is an important factor for a reaction type chemosensor, so the time dependence of RATU to Hg^{2+} was investigated. As shown in Fig. 7, the absorbance and fluorescence intensity almost increased to the maximum within about 60 min and then approximately leveled off, while that of the blank solution was stable at a very low level. The result indicates the reliability and efficiency of RATU for the detection of Hg^{2+}.

3.6. Mechanism for RATU sensing Hg^{2+}

To explore the sensing mechanism of RATU for Hg^{2+}, Job's plot experiments were performed (Fig. 8). A maximal increment of the fluorescence intensity between RATU and RATU-Hg^{2+} appeared at 0.67 (Hg^{2+} molar fraction). According to $n = x/(1-x)$, in which x is the molar fraction of Hg^{2+} corresponding to the maximal fluorescence change and n is the binding stoichiometry, 0.67 indicates the formation of a 1:2 complex between RATU and Hg^{2+}.

The strong fluorescence of RATU-Hg^{2+} in CH_3CN/H_2O (1/99, v/v) could not be quenched by excess EDTA (Fig. 9), indicating that the reaction of RATU with Hg^{2+} was chemically irreversible.

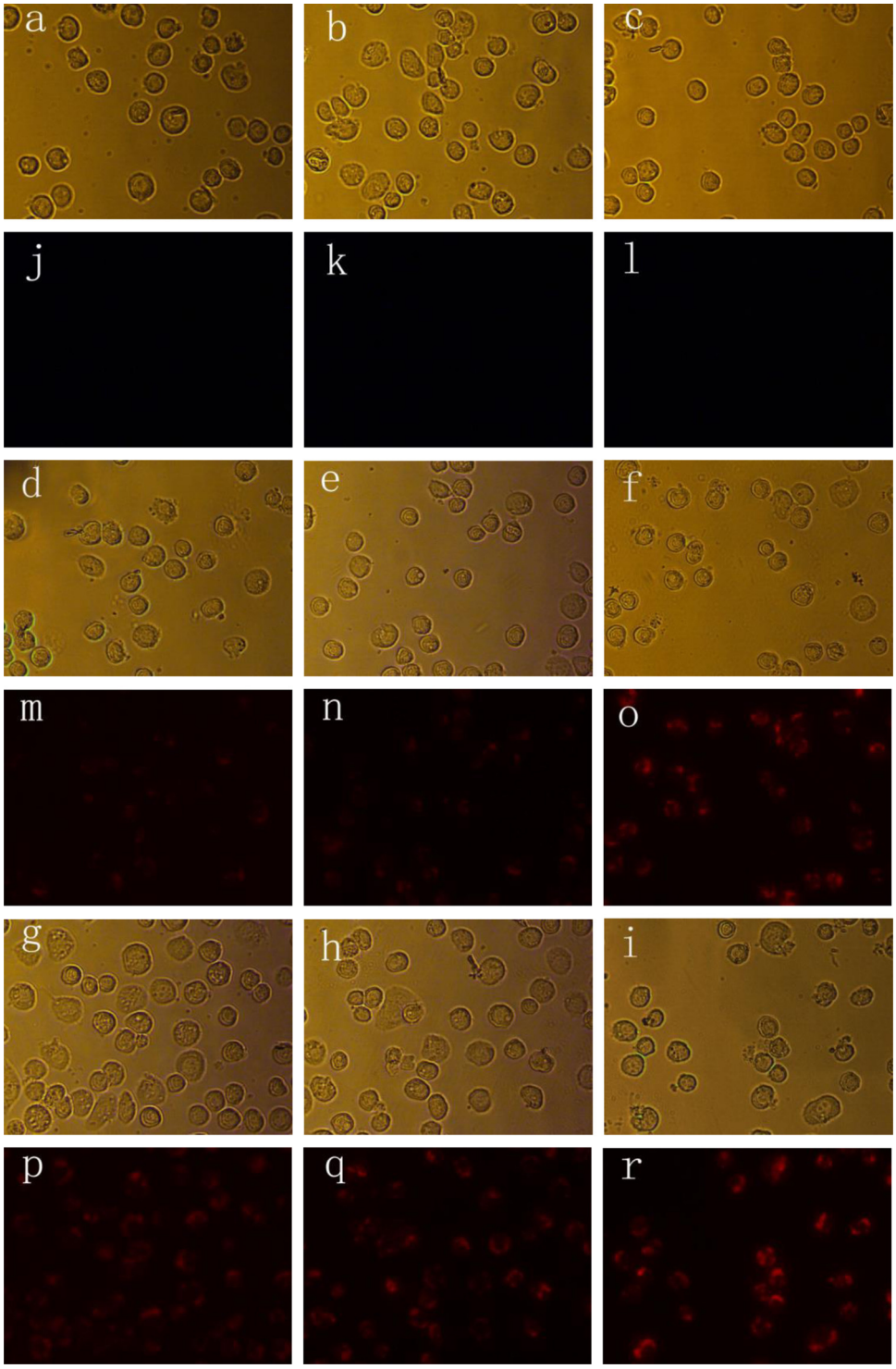

Fig. 14. Images of cells. (a–i) bright-field images; (j–r) fluorescence images of (a–i). (a and j) Blank; (b and k) Hg^{2+} (12 μM); (c and l) RATU (60 μM); (d and m) RATU (30 μM) and Hg^{2+} (9 μM); (e and n) RATU (45 μM) and Hg^{2+} (9 μM); (f and o) RATU (60 μM) and Hg^{2+} (9 μM); (g and p) RATU (30 μM) and Hg^{2+} (12 μM); (h and q) RATU (45 μM) and Hg^{2+} (12 μM); (i and r) RATU (60 μM) and Hg^{2+} (12 μM).

On the basis of the Job's plot and reversibility experiment, a possible model for RATU binding Hg^{2+} was proposed as Scheme 2. Hg^{2+} was first bound to the S atom of thiourea due to its sulphophile and induced the intramolecular charge transfer and resulted in the ring opening of the rhodamine spirolactam, followed by the removal of HgS and other chemical reactions, as described in the reference [22].

Direct evidence for Scheme 2 was obtained from the LC–MS spectra of RATU-Hg^{2+}. As shown in Fig. 10, a peak at *m*/*z* 1242.7964 corresponded to [RATU + $2Hg^{2+}$] verified a 1:2 RATU-Hg^{2+} complex. The other peak at *m*/*z* 1043.3502, 629.3616, 522.1772 and 315.1834 belonged to [RATU + Hg^{2+} + H^+], [RATU′ + H^+], 1/2[RATU + Hg^{2+} + $2H^+$] and 1/2[RATU′ + $2H^+$], respectively. These results suggest a new interaction way between $Hg^{2+}$and rhodamine-bsed chemosensor, in which one RATU

molecule binds two Hg^{2+} ions to two S atoms, followed by the removal of HgS and phenyl fragment to produce some new structures.

Furthermore, the IR spectra of RATU and RATU-Hg^{2+} were recorded (Fig. 11). Compared to the IR spectrum of RATU, the disappearance of the peak at 1668.38 cm^{-1} (C═O) in the IR spectrum of RATU-Hg^{2+} indicated the opening of the spirolactam ring and the variation of the carbon-oxygen double bond (C═O) to the carbon-oxygen single bond (C—O). The vanishing of the peak at 1118.68 cm^{-1} (C═S) matched the removal of HgS. The shift of the peak from 3352.19 to 3448.63 cm^{-1} and its great enhancement manifested the formation of the —NH_2 groups. At the same time, the peaks between 1636 and 1467 cm^{-1} (corresponding to the phenyl and N—H groups) as well as the peaks from 1398 to 1180 cm^{-1} (related to the C—O and C—N groups) were changed obviously in the IR spectrum of RATU-Hg^{2+}, which is also consistent with the speculation that Hg^{2+} was first bound by S atom, and then HgS and phenyl left to give the new compounds RATU′.

To further elucidate the binding mode of RATU with Hg^{2+}, ^1H NMR spectra of RATU and RATU-Hg^{2+} in CD_3CN-D_2O (2/1, v/v) were tested (Fig. 12). It was found that the proton signals of the benzene ring and the CH_2 between the N atoms apparently shifted downfield. In detail, the shifts for the aromatic H_c, H_d, H_e and H_r was from 6.32–6.39 to 6.41–6.44 ppm, and H_f, H_g, H_h, H_i, H_p and H_q was from 7.03–7.54 to 7.08–7.64 ppm, for the aliphatic H_k, H_l and H_m was from 2.45 to 2.73 ppm, and H_j was from 2.99 to 3.16 ppm. These variation matched the events of Hg^{2+} coordinated with S atom and induced the ringopening of the rhodamine spirolactam. Particularly, the appearance of a new peak at 3.44 ppm in the ^1H NMR spectrum of RATU-Hg^{2+} confirmed the CH_2 coming from C═S in the structure of the intermediate RATU′.

The results of LC–MS, IR and ^1H NMR spectra analysis well supported the proposed sensing mechanism.

3.7. Application in real sample analysis

In order to understand the practicability of RATU, the amount of Hg^{2+} in tap water and pool water were determined by our proposed fluorescence assay method, and the results were listed in Table 1. The data revealed a good agreement between the added and the found concentrations of Hg^{2+}. The recovery was between 98.0% and 102.3%. The relative standard deviation (RSD) of three measurements was less than 1.8%. Thus, the present method could be effectively determined Hg^{2+} in real water samples.

3.8. Application in solid support sensor

White cellulose discs (Watson Group) with a diameter of 10 mm were impregnated with 200 μL of RATU (100 μM) CH_3CN solution and then dried in air at 25 °C to get the white dried discs containing RATU, namely the solid support sensors. After immersing the solid support sensors in 2 mL water solutions including increasing amounts of Hg^{2+} for 60 min, visual color changes from colorless to violet were clearly observed (Fig. 13 top). Therefore, RATU could be supported in low cost simple cellulose for monitoring Hg^{2+} in 100% aqueous solution by the naked eye. This method is really useful for the development of portable and convenient onsite detection of environmental Hg^{2+}. In addition, the solid support RATU sensor binding different amounts of Hg^{2+} exhibited different fluorescent images under an ultraviolet analyzer (Fig. 13 bottom).

3.9. Application in living cell imaging

To demonstrate its potential biological applications, RATU was employed to fluorimetrically detect Hg^{2+} in living cells. No fluorescent signal could be observed in the untreated cells and the cells

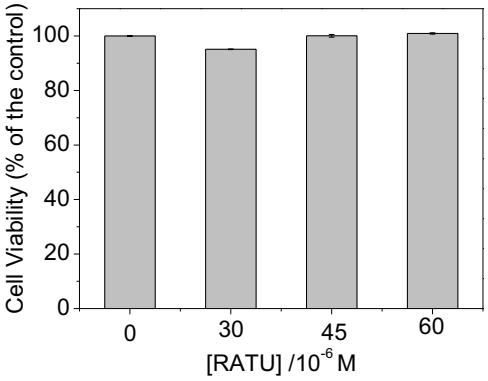

Fig. 15. Viability of sf-9 cells incubated with 0, 30, 45 and 60 μM of RATU.

only treated with RATU (or Hg^{2+}) (Fig. 14j–l). However, the cells incubated with RATU and Hg^{2+} emitted notable red fluorescence (Fig. 14m–r). Breadthwise, from Fig. 14m–o (or Fig. 14p–r), the intracellular fluorescence intensity increased upon raising the concentration of RATU. Lengthways, the intracellular fluorescence of Fig. 14p–r was stronger than that of Fig. 14m–o respectively owing to the higher concentration of Hg^{2+}. The normal shape of the cells in bright field images (Fig. 14a–i) confirmed that the cells were viable during the imaging experiments. These results indicated that RATU could be used for detecting Hg^{2+} in biological samples.

3.10. Cytotoxicity of RATU

Cell viability was evaluated by a MUSE Smart Touch cell analyzer. Taking the viability of the control as 100%, the viability of the cells incubated with 30, 45 and 60 μM of RATU for 24 h was 95.13%, 100.06% and 100.93% respectively (Fig. 15). It can be seen that incubating sf-9 cells with RATU did not greatly negatively affect the cell viability. The slightly dropped viability of the 30 μM RATU-treated cells might be result from the cell itself. Therefore RATU exhibited very low cytotoxicity and could be used for intracellular detection.

3.11. Comparison of RATU with other typical chemosensors

Several so-called water soluble rhodamine-based Hg^{2+} sensors have been reported. They possessed multiple attractive features such as nearly pure water working media, high selectivity and sensitivity, low detection limit and naked-eye observed color changes [27,28]. However, some raw materials, intermediates and sensors are difficult to obtain [29,30], and the anti-interference ability of some sensors is modest or uninvestigated [31,32], and the practical application of other sensors is unknown [33,34]. Besides the advantages like the reported sensors, our newly developed chemosensor has accessible raw materials, wide linear Hg^{2+} concentration range (0–90 μM), favorable working pH span (6.01–8.57), strong interference immunity, low cytotoxicity, good validity for signaling Hg^{2+} in environmental water sample and living cell, and promising prospect in the portable onsite detection of Hg^{2+} in 100% aqueous solution. In addition, the introduction of phenyl isothiocyanate into the chemosensor structure leads to not only the sensor′s high affinity to Hg^{2+} but also a possible new sensing mechanism.

4. Conclusion

In summary, we reported a new rhodamine-bsed turn-on colorimetric and fluorescent Hg^{2+} sensor (RATU) with excellent overall performance, such as nearly pure water working medium, high sensitivity and selectivity, wide linear Hg^{2+} concentration range, low detection limits, strong interference immunity, favorable working

pH span, naked-eye observed color changes, low cytotoxicity and good validity for signaling Hg^{2+} in real water sample and living cell. The fact that the RATU-containing cellulose disc could monitor Hg^{2+} in 100% aqueous solution by the naked eye revealed RATU's promising prospect in the portable onsite detection of Hg^{2+}. Job's plot and reversibility experiments as well as LC–MS, IR and ^1H NMR analysis results infer a new interaction way between Hg^{2+} and RATU which is beneficial to novel rhodamine-bsed chemosensor design.

Acknowledgments

This work was supported by the National Natural Science Foundation of China (21074085), the Priority Academic Program Development of Jiangsu Higher Education Institutions, the Graduate Student Innovation Training Project of Jiangsu Province (KYLX_1241), and the State and Local Joint Engineering Laboratory for Novel Functional Polymeric Materials.

Appendix A. Supplementary data

Supplementary data associated with this article can be found, in the online version, at http://dx.doi.org/10.1016/j.snb.2016.03.125.

References

[1] C.S. Vergilio, C.E.V. Carvalho, E.J.T. Melo, Mercury-induced dysfunctions in multiple organelles leading to cell death, Toxicol. in Vitro 29 (2015) 63–71.
[2] P. Mahato, S. Saha, P. Das, H. Agarwalla, A. Das, An overview of the recent developments on Hg^{2+}recognition, RSC Adv. 4 (2014) 36140–36174.
[3] D.T. Quang, J.S. Kim, Fluoro-and chromogenic chemodosimeters for heavy metal ion detection in solution and biospecimens, Chem. Rev. 110 (2010) 6280–6301.
[4] J.S. Wu, W.M. Liu, J.C. Ge, H.Y. Zhang, P.F. Wang, New sensing mechanisms for design of fluorescent chemosensors emerging in recent years, Chem. Soc. Rev. 40 (2011) 3483–3495.
[5] Y. Yuan, S.G. Sun, S. Liu, X.W. Song, X.J. Peng, Highly sensitive and selective turn-on fluorescent probes for Cu^{2+} based on rhodamine B, J. Mater. Chem. B 3 (2015) 5261–6265.
[6] S. Mandal, A. Banerjee, S. Lohar, A. Chattopadhyay, B. Sarkar, S.K. Mukhopadhyay, A. Sahana, D. Das, Selective sensing of Hg^{2+} using rhodamine–thiophene conjugate: red light emission and visual detection of intracellular Hg^{2+} at nanomolar level, J. Hazard. Mater. 261 (2013) 198–205.
[7] Z.Y. Zhang, S.Z. Lu, C.M. Sha, D.M. Xu, A single thiourea-appended 1,8-naphthalimide chemosensor for three heavy metal ions: Fe^{3+}, Pb^{2+}, and Hg^{2+}, Sens. Actuators B 208 (2015) 258–266.
[8] H.D. Xiao, J.H. Li, K.T. Wu, G. Yin, Y.W. Quan, R.Y. Wang, A turn-on BODIPY-based fluorescent probe for Hg(II) and its biologicalapplications, Sens. Actuators B 213 (2015) 343–350.
[9] S. Yang, W. Yang, Q. Guo, T. Zhang, K. Wu, Y. Hu, A highly selective and ratiometric fluorescence probe for the detection of Hg^{2+} and pH change based on coumarin in aqueous solution, Tetrahedron 70 (2014) 8914–8918.
[10] J. Song, M. Huai, C. Wang, Z. Xu, Y. Zhao, Y. Ye, A new FRET ratiometric fluorescent chemosensor for Hg^{2+} and its application in living EC 109 cells, Spectrochim. Acta A 139 (2015) 549–554.
[11] H.R. Cheng, Y. Qian, Intramolecular fluorescence resonance energy transfer in a novel PDI-BODIPY dendritic structure: synthesis, Hg^{2+} sensor and living cell imaging, Sens. Actuators B 219 (2015) 57–64.
[12] N. Kumar, Rhodamine appended thiacalix[4]arene of 1,3-alternate conformation for nanomolar detection of Hg^{2+} ions, Sens. Actuators B 161 (2012) 311–316.
[13] T.K. Khan, M. Ravikanth, 3-(Pyridine-4-thione)BODIPY as a chemodosimeter for detection of Hg(II) ions, Dyes Pigm. 95 (2012) 89–95.
[14] F.Y. Yan, M. Wang, D.L. Cao, N. Yang, Y. Fu, L. Chen, L.G. Chen, New fluorescent and colorimetric chemosensors based on the rhodamine detection of Hg^{2+} and Al^{3+} and application of imaging in living cells, Dyes Pigm. 98 (2013) 42–50.
[15] J.H. Hu, J.B. Li, J. Qi, J.J. Chen, Highly selective and effective mercury(II) fluorescent sensors, New J. Chem. 39 (2015) 843–848.
[16] X.Q. Chen, T. Pradhan, F. Wang, J.S. Kim, J. Yoon, Fluorescent chemosensors based on spiroring-opening of xanthenes and related derivatives, Chem. Rev. 112 (2012) 1910–1956.
[17] S. Hazra, S. Balaji, M. Banerjee, A. Ganguly, N.N. Ghosh, A. Chatterjee, A PEGylated-rhodamine based sensor for turn-on fluorimetric and colorimetric detection of Hg^{2+} ions in aqueous media, Anal. Methods 6 (2014) 3784–3790.
[18] Z. Cheng, G. Li, M. Liu, A metal-enhanced fluorescence sensing platform based on new mercapto rhodamine derivatives for reversible Hg^{2+} detection, J. Hazard. Mater. 287 (2015) 402–411.
[19] S. Lee, B.A. Rao, Y.A. Son, Colorimetric and "turn-on" fluorescent determination of Hg^{2+} ions based on a rhodamine–pyridine derivative, Sens. Actuators B 196 (2014) 388–397.
[20] A.F. Liu, L. Yang, Z.Y. Zhang, Z.L. Zhang, D.M. Xu, A novel rhodamine-based colorimetric and fluorescent sensor for the dual-channel detection of Cu^{2+} and Fe^{3+} in aqueous solutions, Dyes Pigm. 99 (2013) 472–479.
[21] W. Shi, H.M. Ma, Rhodamine B thiolactone: a simple chemosensor for Hg^{2+} in aqueous media, Chem. Commun. 16 (2008) 1856–1858.
[22] J.S. Wu, I.C. Hwang, K.S. Kim, J.S. Kim, Rhodamine-based Hg^{2+}-selective chemodosimeter in aqueous solution: fluorescent off–on, Org. Lett. 9 (2007) 907–910.
[23] S. Angupillai, J.Y. Hwang, J.Y. Lee, B.A. Rao, Y.A. Son, Efficient rhodamine-thiosemicarbazide-based colorimetric/fluorescent 'turn-on' chemodosimeters for the detection of Hg^{2+} in aqueous samples, Sens. Actuators B 214 (2015) 101–110.
[24] M.H. Lee, H.J. Kim, S. Yoon, N. Park, J.S. Kim, Metal ion induced FRET off–on in tren/dansyl-appended rhodamine, Org. Lett. 10 (2008) 213–216.
[25] Y. Zhou, J. Zhang, L. Zhang, Q. Zhang, T. Ma, J. Niu, A rhodamine-based fluorescent enhancement chemosensor for the detection of Cr^{3+} in aqueous media, Dyes Pigm. 97 (2013) 148–154.
[26] A.K. Mandal, M. Suresh, P. Das, E. Suresh, M. Baidya, S.K. Ghosh, A. Das, Recognition of Hg^{2+} ion through restricted imine isomerization: crystallographic evidence and imaging in live cells, Org. Lett. 14 (2012) 2980–2983.
[27] M. Wang, F.Y. Yan, Y. Zou, N. Yang, L. Chen, L.G. Chen, A rhodamine derivative as selective fluorescent and colorimetric chemosensor for mercury(II) in buffer solution, test strips and living cells, Spectrochim. Acta A 123 (2014) 216–223.
[28] H.N. Kim, S.-W. Nam, K.M.K. Swamy, Y. Jin, X.Q. Chen, Y. Kim, S.J. Kim, S. Park, J. Yoon, Rhodamine hydrazone derivatives as Hg^{2+} selective fluorescent and colorimetric chemosensors and their applications to bioimaging and microfluidic system, Analyst 136 (2011) 1339–1344.
[29] X.L. Chen, X.M. Meng, S.X. Wang, Y.L. Cai, Y.F. Wu, Y. Feng, M.Z. Zhu, Q.X. Guo, A rhodamine-based fluorescent probe for detecting Hg^{2+} in a fully aqueous environment, Dalton Trans. 42 (2013) 14819–14825.
[30] S. Hazra, S. Balaji, M. Banerjee, A. Ganguly, N.N. Ghosha, A. Chatterjee, A PEGylated-rhodamine based sensor for turn-on fluorimetric and colorimetric detection of Hg^{2+} ions in aqueous media, Anal. Methods 6 (2014) 3784–3790.
[31] D. Zhang, M. Li, M. Wang, J.H. Wang, X. Yang, Y. Ye, Y.F. Zhao, A rhodamine-phosphonate off–on fluorescent sensor for Hg^{2+} in natural water and its application in live cell imaging, Sens. Actuators B 177 (2013) 997–1002.
[32] X. Zhang, Y.Y. Zhu, A new fluorescent chemodosimeter for Hg^{2+}-selective detection in aqueous solution based on Hg^{2+}-promoted hydrolysis of rhodamine-glyoxylic acid conjugate, Sens. Actuators B 202 (2014) 609–614.
[33] X. Zhang, X.J. Huang, Z.J. Zhu, A reversible Hg(II)-selective fluorescent chemosensor based on a thioether linked bis-rhodamine, RSC Adv. 3 (2013) 24891–24895.
[34] S. He, Q.C. Liu, Y.Y. Li, F.F. Wei, S.T. Cai, Y. Lu, X.S. Zeng, Rhodamine 6G-based chemosensor for the visual detection of Cu^{2+} and fluorescent detection of Hg^{2+} in water, Chem. Res. Chin. Univ. 30 (2014) 32–36.

Biographies

Miaomiao Hong is currently working toward a M.S. degree in College of Chemistry, Chemical Engineering and Materials Science, Soochow University.

Xiangyu Lu was an undergraduate in College of Chemistry, Chemical Engineering and Materials Science, Soochow University when she participated in the work.

Yuhua Chen is currently working as an associate professor in College of Pre-clinical Medical and Biological Science, Soochow University.

Dongmei Xu is currently working as a professor in College of Chemistry, Chemical Engineering and Materials Science, and Jiangsu Key Laboratory of Advanced Functional Polymer Design and Application, Soochow University.